

# Analysis of the Current Density Distribution in OPGW Cables under Lightning Conditions Using the BOR-FDTD Method

*Kellen Diane de Carvalho Gomes<sup>1</sup>, Tiago Carvalho Martins<sup>1</sup>, João Tavares Pinho<sup>1</sup>, Victor Dmitriev<sup>1</sup>, Sérgio Colle<sup>2</sup>, Marcelo de Araújo Andrade<sup>3</sup>, João Carlos Vieira da Silva<sup>3</sup>, Mauro Bedia<sup>3</sup>*

1. Universidade Federal do Pará - Belém, Pará, Brazil - +55-91-3201-7299 - jtpinho@ufpa.br

2. Universidade Federal de Santa Catarina - Florianópolis, Santa Catarina, Brazil

3. Prysmian Cabos e Sistemas do Brasil - Sorocaba, São Paulo, Brazil

## Abstract

This paper analyzes the current density distribution in OPGW cables subjected to lightning conditions using Maxwell's equations discretized by the numerical method known as "body of revolution – finite difference time domain" (BOR-FDTD) using the "Perfectly Matched Layer" (PML) as absorbing condition.

**Keywords:** OPGW cable; Lightning; BOR-FDTD; Perfectly Matched Layer.

## 1. Introduction

With the increasing demand for energy and the growing need for data transmission, a higher level of reliability in electrical and telecommunications systems is required. As a result, companies are improving their products and services, planning and expanding new technologies in their facilities.

The optical cables were usually installed buried in the ground. Aiming at cost reduction, the OPGW technology was developed, which substitutes the conventional ground wire, providing both protection against lightning to the transmission lines and a channel for data transmission.

The study on OPGW cables under lightning conditions is important because of the high incidence of atmospheric discharges in Brazil, which can damage the cables and cause the failures to the electric power systems.

The goal of this paper is to calculate the current density distribution on the cross section of different cables under lightning conditions.

## 2. The OPGW Cable

The structure of the OPGW cable is basically formed by a dielectric core, where the optical fibers are located, an aluminum tube that protects the fiber package, and a frame formed by conductor wires. These wires that form the frame can be made of aluminized steel, galvanized steel or aluminum alloy [1].

To evaluate the behavior of the current density in the wire and allow for a simple analysis and computational implementation, the structure was modeled as being formed by three homogeneous layers, as shown in Figure 1.

Layer 1 represents the dielectric core with the optical fibers; layer 2 is the aluminum tube and layer 3 is the cable's frame, which is normally made of galvanized steel.

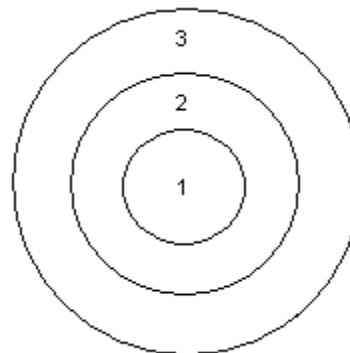


Figure 1. Cross-section for the model of the OPGW

## 3. Lightning Analysis

Lightning is a phenomenon that consists of a high intensity electric discharge occurring in the atmosphere, which happens due to the electrification of the clouds in thunderstorms. Its destructive power is enormous, being one of the major causes for damaging the OPGW cables, as observed in many systems [2].

When the OPGW is hit by lightning three effects may take place:

1. The cable suffers minor damage and, after inspection, it can continue operating normally;
2. The cable suffers severe damage and needs to be repaired. Such procedure usually uses repair rods, which makes the procedure expensive;
3. The cable suffers irreversible damage and needs to be replaced, making the incident even more expensive.

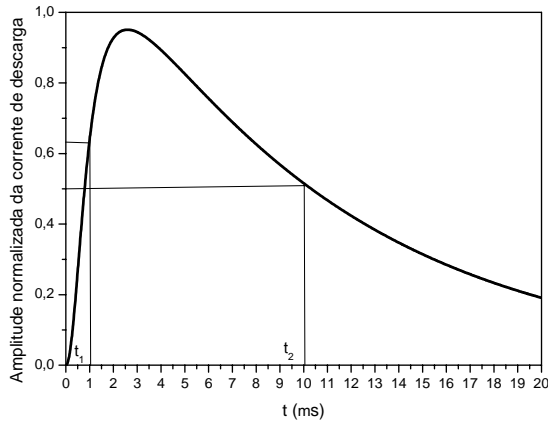
The atmospheric discharge can damage both the metallic wires which constitute its frame, and its optical fibers core, damaging the protection system for power lines, as well as the data transmission system. Therefore, the study of such cables is important to prevent electrical energy and communication systems from failure.

Figure 2 shows an OPGW that was stroke by lightning.



**Figure 2. OPGW cable damaged by lightning**

Knowing that an important parameter of lightning is its current waveform, an analytical expression to simulate the discharge by means of the Heidler Function was used, in which their variables can be adjusted independently [3]. Figure 3 shows an example of this function.



**Figure 3. Heidler Function**

The Heidler Function is represented by the analytical expressions of equations 1 and 2, which reproduce with a very good approximation the curves of return current of an atmospheric discharge.

$$i(t) = \frac{I_0}{\eta} \cdot \frac{(t/\tau_1)^n}{1 + (t/\tau_1)^n} \exp(-t/\tau_2) \quad (1)$$

where

$$\eta = \exp\left[-\left(\tau_1/\tau_2\right)\left(n\tau_1/\tau_2\right)\right]^{(1/n)} \quad (2)$$

and:

$I_0$  – current amplitude;

$\tau_1$  – constant related to the current wave-front time;

$\tau_2$  – constant related to the current wave-drop time;

$\eta$  – amplitude's correction factor;

$n$  – power (2 to 10).

The constants  $I_0$ ,  $\tau_1$  and  $\tau_2$  were chosen based on typical values of the discharge waves found in the literature [4].

Other important parameters are the wave times, such as: wave-front time, half-wave time and total discharge duration:

- Wave-front time is the time between the beginning of the discharge current pulse until the value of its first peak;
- Half-wave time is the elapsed time from the beginning of the discharge current pulse until a 50% reduction of its first peak value;
- Total discharge duration is the elapsed time from the beginning of the discharge current pulse until it equals zero.

To run the simulations for the current impulses some wave-front time and total discharge duration values were chosen, based on values found in the literature [4].

#### 4. The BOR-FDTD Method

The use of numerical techniques to solve electromagnetic problems has become very common due to the increase of the computers processing capacity.

One of the most widely used methods is the finite difference time domain (FDTD), which solves Maxwell's Equations in the time domain. Since in this work, the object of study is a structure with rotational symmetry, cylindrical coordinates were used associated with the "body of revolution" technique (BOR) because this requires less computer memory and its implementation is simpler than FDTD in cylindrical coordinates without the use the BOR.

The BOR-FDTD method is a bi-dimensional formulation of the FDTD using cylindrical coordinates. The fields with azimuthal dependence are expressed as a Fourier Series and, since the azimuthal variations are analytic accounted for, there is no discretization in the  $\phi$ -direction.

The electromagnetic fields in the  $\phi$  direction are given below:

$$\vec{E} = \sum_{m=0}^{\infty} (\vec{e}_u \cos m\phi + \vec{e}_v \sin m\phi) \quad (3)$$

$$\vec{H} = \sum_{m=0}^{\infty} (\vec{h}_u \cos m\phi + \vec{h}_v \sin m\phi), \quad (4)$$

where:

$m$  – number of modes;

$u$  – Fourier coefficient of cosine dependence;

$v$  – coefficients of sine dependences.

The derivation for the updating equations of the BOR-FDTD comes from the Maxwell's Rotational Equations.

$$\nabla \times \vec{E} = -\frac{\partial \mu \vec{H}}{\partial t} + \sigma^m \vec{H} \quad (5)$$

$$\nabla \times \vec{H} = -\frac{\partial \epsilon \vec{E}}{\partial t} + \sigma^e \vec{E} \quad (6)$$

where:

$\varepsilon$  - electric permittivity;  
 $\mu$  - magnetic permeability;  
 $\sigma^e$  - electric conductivity;  
 $\sigma^m$  - magnetic conductivity.

The body of revolution time-domain finite difference method consists of the discretization of the partial derivatives of Maxwell's Rotational Equations. These partial derivatives are substituted by algebraic approximations, based on the central derivative definition. The time is also discretized and the components of the electric and magnetic fields are updated alternately at each time step using the "leapfrog" technique [5], as shown in Figure 4.

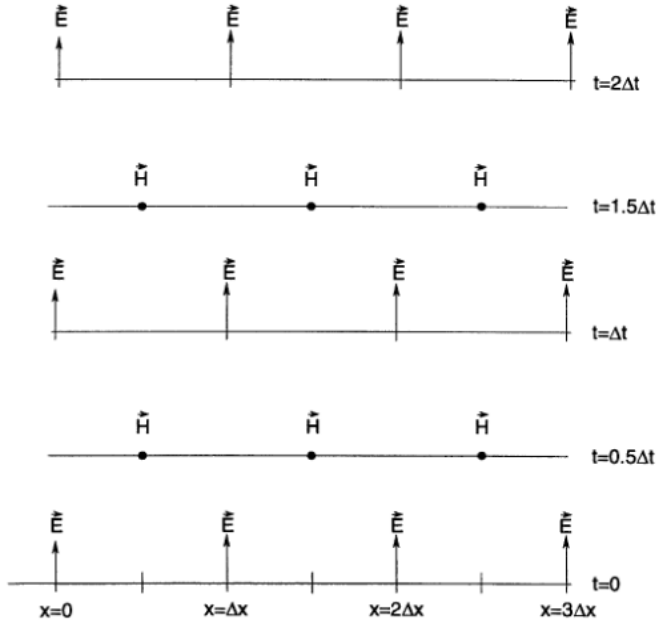


**Figure 4. The "Leapfrog" technique: interspersed distribution in time and space of the component for one-dimension propagation of the Yee algorithm [5]**

The following  $E_z$ ,  $E_r$  e  $H_\phi$  are used:

$$E_r^{n+1}(i,j) = \left( \frac{1 - \frac{\sigma_r^e \Delta t}{2\varepsilon_0 \varepsilon_r}}{1 + \frac{\sigma_r^e \Delta t}{2\varepsilon_0 \varepsilon_r}} \right) E_r^n(i,j) - \left( \frac{\frac{\Delta t}{\varepsilon_0 \varepsilon_r}}{1 + \frac{\sigma_r^e \Delta t}{2\varepsilon_0 \varepsilon_r}} \right) \left[ \frac{H_\phi^{n+1/2}(i,j) - H_\phi^{n+1/2}(i,j-1)}{\Delta z} - mH_z^{n+1/2}(i,j) / (i)\Delta r \right] \quad (7)$$

$$E_z^{n+1}(i,j) = \left( \frac{1 - \frac{\sigma_z^e \Delta t}{2\varepsilon_0 \varepsilon_z}}{1 + \frac{\sigma_z^e \Delta t}{2\varepsilon_0 \varepsilon_z}} \right) E_z^n(i,j) + \left( \frac{\frac{\Delta t}{\varepsilon_0 \varepsilon_z}}{1 + \frac{\sigma_z^e \Delta t}{2\varepsilon_0 \varepsilon_z}} \right) \left[ \frac{\Delta r(i)H_\phi^{n+1/2}(i,j) - \Delta r(i-1)H_\phi^{n+1/2}(i-1,j)}{(i-1/2)\Delta^2 r} + mH_r^{n+1/2}(i,j) / (i-1/2)\Delta r \right] \quad (8)$$

$$H_\phi^{n+1/2}(i,j) = H_\phi^{n-1/2}(i,j) - \left( \frac{\Delta t}{\mu_0} \right) \left[ \frac{E_r^n(i,j+1) - E_r^n(i,j)}{\Delta_z} - \frac{E_z^n(i+1,j) - E_z^n(i,j)}{\Delta_r} \right] \quad (9)$$

where:

$n$  - time index;

$i$  - cell position in the radial direction;

$j$  - cell position in the  $z$  direction;

$\Delta t$  - time discretization;

$\Delta_z$  - spatial discretization in the  $z$  direction;

$\Delta_r$  - spatial discretization in the radial direction.

The spatial and temporal index of the discretized equations follows the Yee cell displacement for cylindrical coordinates [5]. Figure 5 shows the relationship of the components in the plane  $r$ - $z$ .

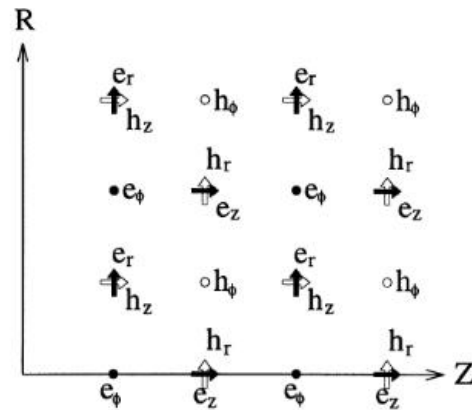


**Figure 5. Field components spatial relations near the  $z$  axis [5]**

The absorbing boundary condition was implemented by the "split-field PML" technique in BOR-FDTD algorithm [5].

## 5. Results

To validate the developed program, a comparison was made with the results of [1] using a 200 kHz sinus waveform as excitation. This comparison is shown in Figure 6.

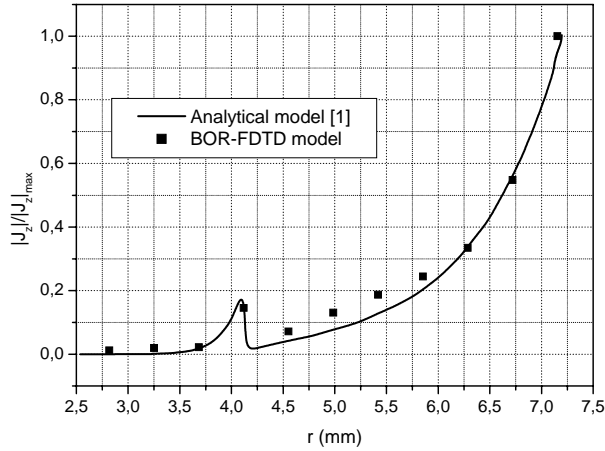


**Figure 6. Comparison between the current density distribution obtained by the present method and the analytical method of reference [1]**

The code was implemented in FORTRAN 77 language for cables of different radii. The radii of the simulated cables are 5.66 mm and 7.47 mm, and the spatial discretization  $\Delta r = \Delta z = 0.4533 \times 10^{-3}$ . The parameters shown in Table 1 were considered for each layer.

**Table 1. Cable parameters**

Layer	Material	Conductivity $\gamma$ (S/m)	Relative permittivity	Relative permeability
1	Silica	0	3.8	1
2	Aluminum	$3.96 \times 10^7$	1	1
3	Steel	$0.2 \times 10^7$	1	1

In the BOR-FDTD implementation, the cable was modeled in the  $r$ - $z$  plan, as shown in Figure 7, being  $n_z$  the number of cells representing the cable length, and  $n_r$  the number of cells representing the cable radius.

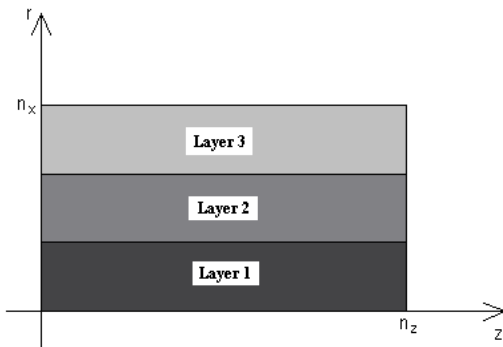


**Figure 7. Cable implementation in the  $r$ - $z$  plane**

The results of the current density shown in Figures 8 and 9 were obtained from the simulation of two different cables, applying discharge pulses with durations of  $\tau_1 = 0.7 \mu\text{s}$  and  $\tau_2 = 105 \mu\text{s}$  through the Fourier Transform, considering a frequency range ranging from 0.1 MHz to 1.5 MHz.

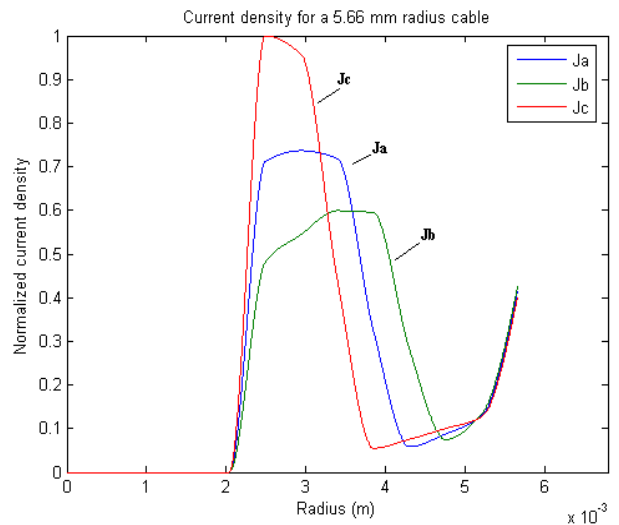
For each of the analyzed cables, the aluminum and the steel layer thicknesses were varied according to the values specified in Tables 2 and 3. The applied current was normalized for a faster convergence of the algorithm.

Table 2 shows the current density  $J_a$  obtained for the cable considering the thickness of the aluminum layer equal to that of steel, and for the  $J_b$  and  $J_c$  cases, the aluminum and steel layers have different thicknesses: for  $J_b$  the aluminum layer is thicker than that of steel, and for  $J_c$  the steel layer is the thickest one. In Table 3  $J_a$ ,  $J_b$  and  $J_c$  are also shown, however with the thicknesses of the aluminum and the steel layers different from each other.

It is observed from Figures 8 and 9 that the current density is distributed along the cross section of the cable and it has a higher concentration in the aluminum layer, regardless of the thickness of the aluminum layer being bigger or smaller than that of the steel layer. This is due to the fact that the aluminum layer has a greater conductivity than the steel layer.

**Table 2. Thickness for each layer of the 5.66 mm radius cable**

Current density	Layer 1	Layer 2	Layer 3
$J_a$	2.04 mm	1.81 mm	1.81 mm
$J_b$	2.04 mm	2.26 mm	1.36 mm
$J_c$	2.04 mm	1.36 mm	2.26 mm



**Figure 8. Current densities for a 5.66 mm radius cable**

**Table 3. Thickness for each layer of the 7.47 mm radius cable**

Current	Layer 1	Layer 2	Layer 3
---------	---------	---------	---------

density			
Ja	2.94 mm	1.36 mm	3.17 mm
Jb	2.94 mm	2.72 mm	1.81 mm
Jc	2.94 mm	1.81 mm	2.72 mm

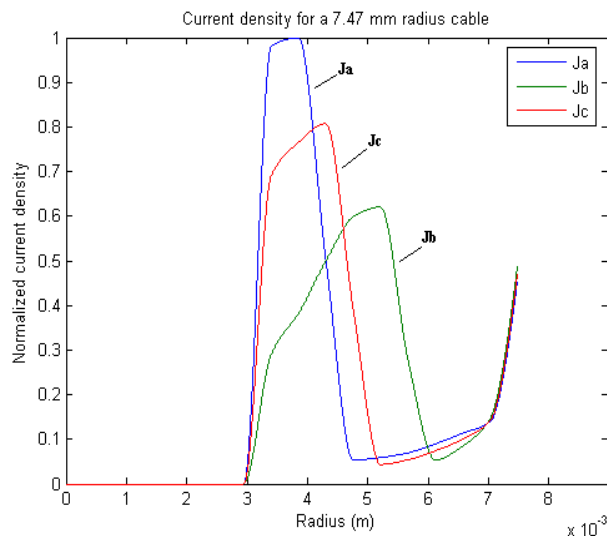


Figure 9. Current density for a 7.47 mm radius cable

## 6. Conclusion

This paper evaluated the behavior of current density distribution in the OPGW cable subjected to a lightning pulse, using the BOR-FDTD method.

The results showed that the current density is distributed with higher concentration in the aluminum layer, due to its larger conductivity. The magnitude of the current varies with the thickness of the layer, a thinner layer having a larger intensity than a thicker layer. Therefore, the results show the importance of proper scaling the thickness of the aluminum layer, to avoid having a very high current concentration in a thin layer, thereby damaging the cable when subjected to lightning strokes.

## 7. References

- [1] - K. Q. da Costa, V. Dmitriev, J. T. Pinho, S. Colle, L. Gonzalez, M. A. Andrade, J. C. V. da Silva, and M. Bedia, "Analytical Model for Calculation of Current Density Distributions Over Cross-section of a Multi-conductor Cable", *IWCS/Focus Conference*, Providence, USA, (2006).
- [2] - M. G. Alvim et al. "Cabo OPGW - Desempenho quanto a Descargas Atmosféricas". XVI SNPTEE, Campinas, Brazil, (2001).
- [3] - S. Visacro Filho, "Descargas Atmosféricas: Uma Abordagem de Engenharia", Artliber, (2005).
- [4] - W. A. Chisholm; J. P. Levine; P. Chowdhuri. "Lightning Arc Damage to Optical Fiber Ground Wires (OPGW): Parameters and Test Methods", IEEE, (2001).

[5] - A. Taflove, "Computational Electrodynamics: The Finite-Difference Time-Domain Method", Artech House, (2000).



Kellen Diane de Carvalho Gomes was born in Santarém, Pará, Brazil in 1980. She graduated in Electrical Engineering at Universidade Federal do Pará (UFPA) in May of 2006. She is now a postgraduate student at UFPA.



Tiago Martins received the M.Sc. degree in Electrical Engineering in 2007 from the Universidade Federal do Pará (UFPA). In 2007 he becomes a D.Sc. student at Pós-graduação em Engenharia Elétrica da Universidade Federal do Pará (PPGEE). Currently, he is focused in the development of computational tools for analysis of electromagnetic scattering by objects covered by plasmonic materials.



João Tavares Pinho was born in Belém, Pará, Brazil, on August 22, 1955. He received the B.Sc. degree in electrical engineering from the Universidade Federal do Pará (Brazil) in 1977, the M.Sc. degree in electrical engineering from the Pontificia Universidade Católica do Rio de Janeiro (Brazil) in 1984, and the Dr.-Ing. degree in electrical engineering from the Rheinisch-Westfälische Technische Hochschule Aachen (Germany) in 1990. He has been with the Department of Electrical Engineering of the Universidade Federal do Pará since 1978, has worked as an assistant at the RWTH Aachen, was the coordinator of the post-graduation course in electrical engineering at the UFPA from 1992 to 1994, and is presently a full professor and leader of a research group on energy alternatives and microwave applications.

Prof. Pinho is ad hoc advisor for several committees and institutions in Brazil, member of various scientific societies, and presently president of the International Solar Energy Society - Brazilian Section, and of the Brazilian Solar Energy Association.



Victor Dmitriev was born in Russia, in 1947. Currently, he is a professor at the Federal University of Para, Belem, Brazil. Dr. Victor Dmitriev has more than 120 papers in scientific journals, several books and patents. The fields of his scientific interest are microwave, millimeter wave and optic components, application of group theory to electromagnetic problems, complex media, nanophotonics, and mathematical methods of electromagnetic theory.



Prof. Sergio Colle  
LEPTEN – Department of Mechanical Engineering – UFSC (Federal University of Santa Catarina)  
Bibliography:

Mechanical Engineer degree in 1970 – UFSC

Master of Science in Mechanical Engineering in 1972 – COPPE / University of Rio de Janeiro  
Doctor of Science in Mechanical Engineering in 1976 – COPPE / University of Rio de Janeiro

Professor of Thermodynamics, Heat Transfer and Solar Energy – Department of Mechanical Engineering – UFSC since 1974

He is presently head of LEPTEN.



Marcelo de Araujo Andrade was born in Florianópolis – SC – Brazil in 1965. He graduated in Mechanical Engineer from Universidade Federal de Santa Catarina in 1988. He joined Prysmian Telecomunicações Cabos e Sistemas do Brasil in 1988 and actually he is in charge of Comercial and R&D Direction.



João Carlos Vieira da Silva was born in São Paulo – SP – Brazil in 1959. He graduated in BSc Physics from Universidade de São Paulo in 1982 and Electrical Engineer from Faculdade de Engenharia de Sorocaba in 1991. He joined Prysmian Telecomunicações Cabos e Sistemas do Brasil in 1977 and actually he is in charge of Product Engineering Department.



Mauro Bedia Jr. was born in São Paulo – SP – Brazil in 1970. He graduated in Mechanical Engineer from Faculdade Santa Cecília in 1996. He joined Prysmian Telecomunicações Cabos e Sistemas do Brasil in 1989 and actually he is responsible for OPGW and ADSS cable development.